Large-Scale Training of Graph Neural Networks for Optimal Markov-Chain Partitioning Using the Kemeny Constant

Sam Alexander Martino¹, João Morado¹, Chenghao Li¹, Zhenghao Lu¹, and Edina Rosta^{1*}

ABSTRACT

The recent trend in using network and graph structures to represent a variety of different data types has renewed interest in the graph partitioning (GP) problem. This interest stems from the need for general methods which can both efficiently identify network communities and reduce the dimensionality of large graphs while satisfying various application-specific criteria. Traditional clustering algorithms often struggle to capture the complex relationships within graphs and generalise to arbitrary clustering criteria. The emergence of graph neural networks (GNNs) as a powerful framework for learning representations of graph data provides new approaches to solving the problem. Previous work has shown GNNs to be capable of proposing partitionings using a variety of criteria, however, these approaches have not yet been extended to work on Markov chains or kinetic networks. These arise frequently in the study of molecular systems and are of particular interest to the biochemical modelling community. In this work, we propose several GNN-based architectures to tackle the graph partitioning problem for Markov Chains described as kinetic networks. This approach aims to minimize how much a proposed partitioning changes the Kemeny constant. We propose using an encoder-decoder architecture and show how simple GraphSAGE-based GNNs with linear layers can outperform much larger and more expressive attention-based models in this context. As a proof of concept, we first demonstrate the method's ability to cluster randomly connected graphs. We also use a linear chain architecture corresponding to a 1D free energy profile as our kinetic network. Subsequently, we demonstrate the effectiveness of our method through experiments on a data set derived from molecular dynamics. We compare the performance of our method to other partitioning techniques such as PCCA+. We explore the importance of feature and hyperparameter selection and propose a general strategy for large-scale parallel training of GNNs for discovering optimal graph partitionings.

Keywords: Graph Neural Networks, Markov chains, Molecular Dynamics, Kemeny Constant

1 INTRODUCTION

Markov chains (MCs), and their extensions, have become a key tool across multiple domains to model dynamical systems^{1,2}. In their simplest form, MCs incorporate sequential data as a Markovian process into a stochastic model, where the probability of observing the next event depends solely on the preceding event. By eliminating the long timescale dependencies that often occur in complex systems, MCs offer a robust and formal method to interpret high-dimensional datasets in the emergent era of big data. The simplicity, transferability, and capability of MCs reduce the difficulties associated with modelling and interpreting ordered dynamics, and have led to a wide range of use cases. These applications encompass modelling character sequences in computer science and genomics^{3,4}, predicting web-user activity⁵, and modelling time-dependent processes in physics and chemistry^{6,7}, to name just a few.

A field that has widely adopted these techniques is computational biochemistry, where the Markov State Model (MSM) formalism has emerged as a strategy for interpreting the results of molecular dynamics (MD) simulations as transitions between aggregated conformational states^{8,9,10}. The surge in popularity of MSMs mirrors researchers' increased ability to quickly generate large quantities of MD data, providing

¹Department of Physics and Astronomy, University College London

^{*}Correspondence: e.rosta@ucl.ac.uk

a useful tool to condense massive data sets into a small and intuitive probabilistic format. MSMs offer intuitive descriptions of complex dynamic systems as transitions between stable minima and unstable transition states¹¹, helping to elucidate the underlying functional kinetics of interest^{12,13}. Over the past few decades, research in this community has led to several domain-specific advances in developing techniques to automatically generate MSM representations of molecular systems. Simultaneously, these techniques have been employed to further sample the multitude of different configurations of biomolecular systems^{14,15}.

Despite being smaller than the huge data sets they originate from, many MSMs remain high-dimensional, consisting of potentially hundreds of states. This large number of states is often unmanageable for downstream tasks such as drug design and biomolecular engineering ¹⁶. As size often becomes the limiting factor to establishing an intuitive understanding of systems, many different approaches have been proposed to reduce the size of MCs and generate optimal ones ^{17,18,19,20}. However, our ability to generate large data sets is only increasing, as modern coarse-graining protocols ²¹ and new developments in machine learning ²² allow for larger time scales to be probed. Traditional graph partitioning algorithms, such as spectral clustering, k-means, or multi-level methods, and their derivatives, have been widely employed to address this problem ^{23,24,25}. However, these algorithms often face limitations in capturing the complex and intricate dependencies on global structure in MCs. Additionally, the generality of these methods means they often disregard the critical dynamic information held within MCs. Alternative Markov-Chain Monte Carlo (MCMC) approaches have been applied for dimensionality reduction on MCs, which can be used with most clustering criteria ^{26,27,28}. Nevertheless, these approaches encounter difficulties in efficiently sampling the most relevant regions of partitioning space, resulting in impractical computation times and frequently overlooking the most optimal solutions.

In this paper, we build upon previous work²⁹ to create a general methodology for reducing the dimensionality of MCs, leveraging recent developments in Machine Learning (ML), where Graph Neural Networks (GNNs) are applied to solve the more general graph partitioning (GP) problem^{30,31,32}. Although several existing approaches use GNNs to minimise partitioning cuts³³ or modularity³⁴, these applications do not extend to kinetic graphs or dynamical criteria. Additionally, these approaches mostly focus on providing approximate partitionings for large graphs rather than exploring their potential for identifying optimal partitionings in smaller networks. We extend these methods by representing MCs as kinetic networks and show how performing gradient descent on a large number of randomly initialised small GNNs can yield optimal network partitionings using elaborate optimization criteria. As a metric to quantitatively assess the degree to which a clustering preserves the underlying dynamics of the MSM, we use the change of Kemeny constant (KC). KC is an inherently dynamical quantity derived from the Mean First Passage Times (MFPTs) associated with any kinetic network, including those used within computational biochemistry³⁵. The proposed MC clustering method can produce a faithful low-dimensional replication of a system's underlying dynamics, while also providing a quantifiable measurement related to the amount of kinetic information lost. Along with outlining a general strategy for the large-scale training of GNNs for graph partitioning, we show our method's performance when minimising the change in KC on several different kinds of synthetic graphs and an example derived from MD simulations. We also test more complex GNN architectures, showing how large-scale training of simple GNNs is the most effective for the task and hypothesizing why this is the case.

2 THEORY

2.1 Graphs

A graph G with N nodes can be represented as a set of vertices $V = \{v_1, ..., v_N\}$ and edges $e_{ij} \in E$, which are often represented as a binary adjacency matrix, \mathbf{A} , where:

$$A_{ij} = \begin{cases} 1, & \text{if } e_{ij} \in E \\ 0, & \text{otherwise} \end{cases}$$
 (1)

Each node, v_i , can be associated with a d_{feat} dimensional feature vector, f_i , similarly admitting a matrix representation as a $(N \times d)$ matrix, \mathbf{F} . These features can be derived from the underlying data or generated

at run time in the case of a featureless graph. This makes it possible to define a general graph structure as:

$$G = (V, E, F) \tag{2}$$

Therefore, in practice, a complete specification of the graph structure can be achieved solely using the matrices $\bf A$ and $\bf F$.

In what follows, the terms clustering, partitioning, and lumping are used interchangeably to refer to the GP problem. The general partitioning problem consists of dividing the nodes of G into M discrete non-overlapping subsets, $s_m \in S$, such that specific criteria are met. These objectives can be general and applicable to nearly all graphs, and include, e.g., optimising connectivity, minimising inter-cluster edges, or maximising intra-cluster similarities. Furthermore, these objectives can also be domain-specific, based on the underlying model the network represents, such as how the KC represents the dynamical information of the system. The $(N \times M)$ partitioning assignment matrix, S, assigns the nodes of G into M distinct states, $\{s_1, \ldots, s_m\}$, where:

$$S_{ik} = \begin{cases} 1, & \text{if } v_i \in s_k \\ 0, & \text{otherwise} \end{cases}$$
 (3)

Since the discrete nature of the assignment matrix poses difficulties for gradient-based methods, it is common to relax this constraint and work with continuous probabilities instead. In practice, this means introducing a soft assignment matrix instead, where S_{ik} now denotes the probability of node v_i belonging to state s_k , subject to the conservation of probability:

$$\sum_{k=1}^{M} S_{ik} = 1 \ \forall \ v_i \in V$$

where k runs over all M possible states.

Two of the most commonly used clustering criteria used for the GP problem are the modularity and the minimum cut, which are defined as follows:

Modularity: The modularity, Q, measures how the connectivity of a graph partitioning differs from what would be expected in a purely random graph with the same node degree distribution. Consequently, this metric provides a quantitative assessment of how statistically surprising a proposed partitioning is, with higher values implying the presence of underlying communities within the data³⁶. The modularity is calculated using the equation:

$$Q = \frac{1}{2m} \sum_{ij}^{N} \sum_{k}^{M} \left[A_{ij} - \frac{d_i d_j}{2m} \right] S_{ik} S_{jk}$$
 (4)

where m is the total number of edges in the graph, d_i and d_j are the node degrees of nodes v_i and v_j , respectively, A_{ij} is given by Eq. (1), and S_{ik} and S_{jk} are given by Eq. (3). While there have been criticisms of the underlying assumptions for modularity, it is a widely used and useful partitioning criterion in many areas 37,38,39 .

Minimum Cut: The minimum cut, C, of a given partitioning is the number of inter-cluster edges, which can be calculated using:

$$C = \sum_{i=1}^{N} \sum_{j \neq i}^{N} \sum_{k=1}^{M} \sum_{l \neq k}^{M} S_{ik} S_{jl} A_{ij}$$
 (5)

Where all indices and matrix values are given as previously defined. The simplicity of this criterion has led to its popularity across multiple domains, spurred on by its proved equivalence to the max-flow criterion⁴⁰. It stands as one of the most studied partitioning criteria^{41,42,43}, alongside its further generalisations commonly used to obtain more balanced clusters with minimal cuts^{44,45}.

2.2 Markov Chains

The dynamical clustering criterion based on KC we used in this paper is derived from the kinetic properties of an MC. In previous work, we explored the relationship between the MFPTs and KC, providing thorough derivations of all the quantities presented below. Here we briefly summarise the key results required and direct the reader to our previous paper for a detailed reference⁴⁶.

In a discrete-time, homogeneous MC comprising of n-states, the probability vector of a random walk occupying any of the n-states at time t, $\mathbf{p}(t)$, can be expressed using a stochastic rate matrix, \mathbf{K} , and a set of initial occupation probabilities, $\mathbf{p}(0)$, such that:

$$\mathbf{p}(t) = e^{\mathbf{K}t}\mathbf{p}(0) \tag{6}$$

Where $t=l\tau$, since in the discrete case moves between states happen at multiples $l=1,2,\ldots$ of a given time interval τ . The quantity $\mathbf{Q}(t)=e^{\mathbf{K}\tau}$ is known as the Markov matrix, and to ensure the conservation of probability, we have:

$$\sum_{i} K_{ji} = 0, \forall i \tag{7}$$

The matrix \mathbf{K} , or similarly \mathbf{Q} , can be calculated from experimental or simulated transition data, such as MD trajectories, or a series of string-like sequences typically used in genomics. \mathbf{K} fully defines the dynamic properties of the MC and can be used to derive several useful quantities relating to its underlying dynamics. Assuming detailed balance, the spectral decomposition of \mathbf{K} into left, ψ_i^l , and right, ϕ_i^l , eigenvectors and corresponding eigenvalues, λ_l , is given by:

$$\mathbf{K} = \sum_{l=1}^{n} \lambda_l \psi^{(l)} \phi^{(l)} \tag{8}$$

Where the index l orders the eigenvalues in descending order.

This yields real eigenvalues that are upper-bounded by 0. The eigenvector corresponding to the largest right eigenvector, $\psi^{(1)}$, is known as the equilibrium probability and is commonly denoted by \mathbf{p}^{eq} , corresponding to the distribution the system converges to as $t \to \infty$. The other eigenvectors contain useful kinetic information corresponding to the relaxation and mixing times of the MC. These eigenvectors can be used to derive an expression for the average time it takes for a random walk starting from state i to first arrive at state j, i.e., the MFPTs of an MC, denoted t_{ii} :

$$t_{ji} = \frac{1}{p_j^{\text{eq}}} \left[\sum_{l>1} \frac{1}{|\lambda_l|} \psi_j^{(l)} (\phi_j^{(l)} - \phi_i^{(l)}) \right]$$
 (9)

Which can be alternatively expressed in matrix form as:

$$t_{ji} = \frac{1}{p_j^{\text{eq}}} \left[(\mathbf{p}^{\text{eq}} \mathbf{1}_N^T - \mathbf{K})_{jj}^{-1} - (\mathbf{p}^{\text{eq}} \mathbf{1}_N^T - \mathbf{K})_{ji}^{-1} \right]$$
(10)

KC is the surprising result that the sum over all states of the product of the MFPTs with the equilibrium probabilities, p_i^{eq} , is a constant value for all i, i.e:

$$\zeta = \sum_{j} p_j^{\text{eq}} t_{ji} = \sum_{j} \sum_{l>1} \frac{1}{|\lambda_l|} \psi_j^{(l)} (\phi_j^{(l)} - \phi_i^{(l)}) = \sum_{l>1} \frac{1}{|\lambda_l|}$$
(11)

This constant provides an inherently dynamical scalar quantity, ideal for gradient-based optimisation methods. By reintroducing the assignment matrix, S, from Eq. (3), and defining a partitionings lumped equilibrium probability, P_M^{eq} , as simply:

$$P_M^{\text{eq}} = \sum_{i \in M} p_i S_{iM} \tag{12}$$

KC can be redefined in terms of a partitioned MC's KC, ζ_S , and a variational term, such that:

$$\zeta = \zeta_{\mathbf{S}} + \sum_{M} \frac{1}{P_M^{\text{eq}}} \sum_{i,j \in M} p_j^{\text{eq}} p_i^{\text{eq}} t_{ji}$$

$$\tag{13}$$

Rearranging this equation yields provides our partitioning metric ΔK :

$$\zeta - \zeta_{\mathbf{S}} = \Delta K = \sum_{M} \frac{1}{P_{M}^{\text{eq}}} \sum_{i,j \in M} p_{j}^{\text{eq}} p_{i}^{\text{eq}} t_{ji}$$

$$\tag{14}$$

From this equation, it is clear that for the trivial single-state partitioning $M=1, \Delta K=\zeta$, and when M=N, the value of ΔK is 0.

2.3 Graph Neural Networks

To describe GNNs in this work we adopt a message-passing formalism⁴⁷ where a GNN-based encoder maps a node v_i in G to a context-aware embedding using T separate layers via the iterative process:

$$m_i^{t+1} = \sum_{j \in \mathcal{N}(v_i)} M_t(h_i^t, h_j^t, x_{ij})$$

$$h_i^{t+1} = U_t(h_i^t, m_i^{t+1})$$
(15)

Where $t \in \{1, ..., T\}$ denotes the current network depth, $\mathcal{N}(v_i)$ is the local neighbourhood of all nodes connected by edges to node v_i , and h_i^t represents the hidden representation of node v_i at depth t. For consistency, the initial node feature vectors F_i are represented by h_i^0 .

The functions M_t and U_t are commonly implemented as neural networks, known as the message-passing function and vertex update function, respectively. Their exact formula depends on the type of graph layer used.

Two different graph layers are tested in our methodology: the GraphSAGE⁴⁸ and the GATv2⁴⁹ layers. The former was chosen to provide a simpler, lower parameter function, which takes fewer resources to train, while the latter provides a more complex layer with the capability to better attune to all nodes. GraphSAGE layers use a simple message-passing function consisting of either the sum or mean, and a vertex update function which concatenates these expressions and feeds them into a feed-forward neural network.

$$m_i^{t+1} = \begin{cases} \frac{1}{n} \sum_{j \in \mathcal{N}(v_i)} h_j^{t-1}, & \text{if mean} \\ \max_{j \in \mathcal{N}(v_i)} \sigma \left(\mathbf{W}_{\text{pool}} h_j^{t-1} + b \right) & \text{if max} \end{cases}$$
 (16)

$$h_i^{t+1} = \sigma(\mathbf{W}^{\mathbf{k}}[h_i^{t+1}||m_i^{t+1}])$$
(17)

Where $[\cdot||\cdot]$ denotes concatenation and σ is any non-linear function.

GATv2 layers replace this with a formulation based on scaled dot-product attention seen in transformer layers. This differs by performing the aggregation step individually for each node in a neighbourhood to calculate a context-aware attention mask, which is then used to perform a weighted vertex update:

$$m(h_i^t, h_j^t) = \underset{j \in \mathcal{N}(v_i)}{\operatorname{softmax}} \left(\mathbf{a}^T \operatorname{LeakyReLU}(\mathbf{W} \cdot [h_i^t || h_j^t]) \right) \tag{18}$$

$$h_i^{t+1} = \sigma(\sum_{j \in \mathcal{N}(v_i)} m(h_i^t, h_j^t) \cdot \mathbf{W} h_j^t), \tag{19}$$

Which can be generalised across multiple attention heads.

3 METHODOLOGY

The proposed method assumes a given neural network architecture, $\Phi(\theta)$, is sufficiently expressive such that the mappings it explores, from the space of ${\bf F}$ to the space of possible partitionings ${\bf S}^{N\times M}$, includes the optimal solution to the GP problem given our clustering criteria ${\bf S}^{\rm opt}$, along with a region of parameter space which can be optimised via gradient descent to yield it. Taking inspiration from Monte Carlo approaches to similar problems, we look to determine ${\bf S}^{\rm opt}$ by initialising Φ with several different sets of parameters θ and optimizing them in parallel using modern ML tools. In this framework, GNNs are an effective Ansatz to begin partitioning graphs using complex criteria. They also provide a generic and

intuitive optimization framework with gradient descent. As Φ is a general model, operating in $\mathbb R$ without any problem-specific restrictions on its values or gradients, it can yield the trivial solutions to Eq. (14), such as the aforementioned M=N case. To overcome this, we take inspiration from similar work on producing balanced clusters^{33,34}, and additionally optimise including a penalty function, which pushes the network away from trivial solutions and gives the final form of the loss function, \mathcal{L} :

$$\mathcal{L} = \underbrace{\sum_{M} \frac{1}{P_{M}^{\text{eq}}} \sum_{i,j \in M} p_{j}^{\text{eq}} p_{i}^{\text{eq}} t_{ji}}_{\Delta K} + \underbrace{\sum_{j} \frac{\eta}{\sqrt{2\pi\sigma}} \exp\left[-0.5 \left(\frac{\sum_{i} S_{ij}}{\sigma}\right)^{2}\right]}_{\text{Penalty Function}}$$
(20)

Optimal Kemeny constant partitionings can have unbalanced subsets, with clusters that contain only a few nodes often being the most interesting transition states 11 . Therefore the form of the penalty function is designed to penalise for any invalid clustering (where any cluster has zero nodes), while also allowing the network to converge very unbalanced partitions with at least one node. The final penalty function is based on a Gaussian centred on 0, parameterised using $\sigma=1.0$ and $\eta=15$ in this work, meaning the penalty becomes larger as any cluster tends to 0 nodes and is negligible for 1 or more nodes.

As MCs do not fit into the graph structure outlined in Eq. (2), simple methods were derived for interpreting the matrices $\bf A$ and $\bf F$ from MCs. The connectivity of the graph was decided using a naive cutoff method, taking all node pairs (v_i,v_j) with $(Q_{ij}+Q_{ji})/2>c$, where c is a constant. In practice, we found c=0.015 to be sufficient for all graphs we worked with, although in other applications this could be changed depending on the density of the resulting network. A systematic exploration of various node features was undertaken. We tested the adjacency matrix, the rate matrix, the Markov matrix, and the MFPTs, along with a principle component analysis (PCA) of all 3 of these, and the eigenvectors of the rate or Markov matrix which defines the network. We also tested both a simple linear layer which combined them, and finally, a trainable embedding layer, which is often used in dictionaries in large language models⁵⁰.

All neural network architectures tested used a GNN-based encoder, mapping the $d_{\rm feat}$ dimensional features into an embedding dimension $d_{\rm embed}$ via a hidden representation of size $d_{\rm hidden}$. Mean pooling was used for our aggregation function in the GraphSAGE layers as it provided better stability during training. The encoder was then followed by either a series of linear layers or attention layers of dimension $d_{\rm hidden}$ as a decoder⁵¹. The transformer-like attention-based decoder can process a whole clustering at once as a sequence of node embeddings and was chosen to provide another comparison between a simpler model and one which is larger, more expressive, and better suited to deal with highly contextual sequences like the node-cluster assignment matrix. The output of the transformer layers was normalised and added back to the input before being processed by a feed-forward layer, and we used two of these layers with a dropout layer between. For positional encoding, a single trainable graph layer was used to provide global context for the nodes, and allow the network to better discriminate between nodes with similar features. All neural networks used are described in detail in Fig. (1).

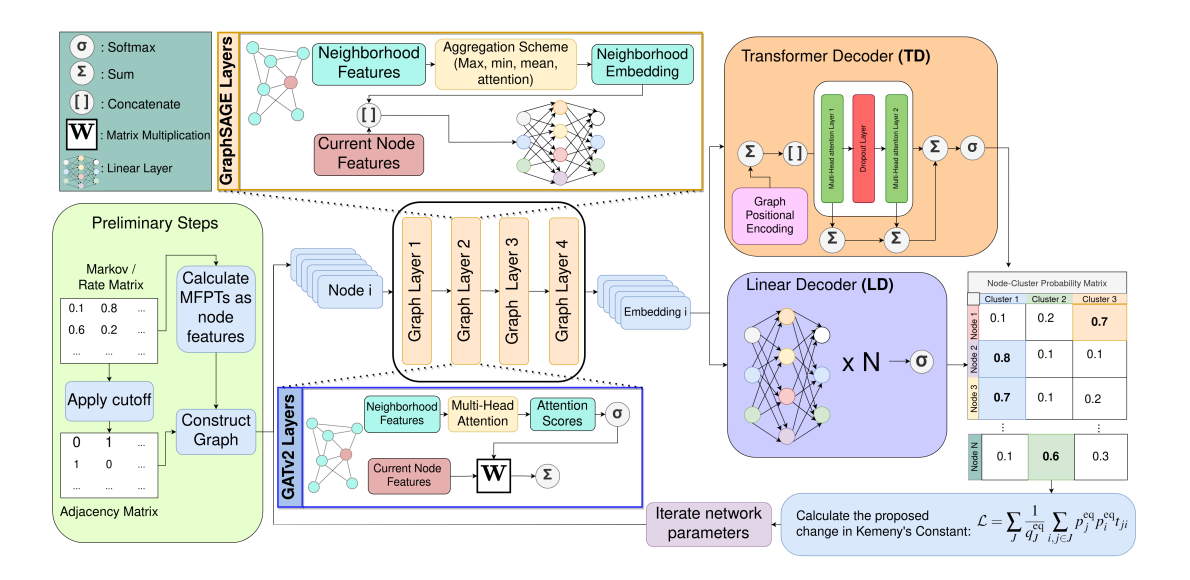


Figure 1. Details of all four GNN architectures used, along with a description of the preprocessing required to begin training, together with an overview of the training loop process for a single gradient optimization step. Implementations of the GraphSAGE and GATv2 GNN layers used in the encoder is provided, along with a schematic description of the transformer decoder (TD) and linear decoder (LD) architectures. Activation functions for the various layers are not included for brevity.

Building on the simplest model with GraphSAGE layers and the linear decoder (GraphSAGE + LD), we validated this model and extended it in two directions to test whether more complex architectures could improve performance. Besides the GraphSAGE encoder, we also implemented the GATv2 encoder. In addition to the linear decoder, we also implemented a transformer decoder (TD). This results in four models: (i) GraphSAGE layers and the linear decoder (GraphSAGE + LD), (ii) linear decoder with GATv2 layers (GATv2 + LD), (iii) GraphSAGE with transformer decoder (GraphSAGE + TD), and finally (iv) GATv2 with transformer decoder (GraphSAGE + TD).

To enable fast and efficient training of the networks, a general parallel methodology for training GNNs for partitioning was established, outlined in Fig. (2). This requires three additional functions to be defined, as well as a valid loss function and the number of processes P:

Generator Function \mathcal{I} : This function returns valid parameters θ for a given neural network Φ . This provides the initial starting point in parameter space for optimisation, and complex generators can be used to provide a quicker convergence. In this work, however, simple initialisation using both the Kaiming and Glorot algorithms were tested, before settling on using Glorot due to its slight advantage observed in early tests. 52,53

Culling Function C: This function determines whether or not a worker thread has finished training a network, and is called after a predetermined number of optimisation steps has finished. Observing individual runs, it is common to see neural networks which initialise in local minima of parameter space and are unable to be trained. An effective culling function allows for these types of runs to be terminated early, allowing for more time to be spent in interesting regions of parameter space. To show the validity of the method, all experiments in this paper terminate after a predetermined number of training steps.

Termination Function \mathcal{T} : This function determines when to stop training, and when combined with effective choices for \mathcal{I} and \mathcal{C} , can allow for the implementation of complex methodologies for determining the convergence of an experiment.

This methodology aims to be as general as possible to make implementing future applications for different criteria straightforward.

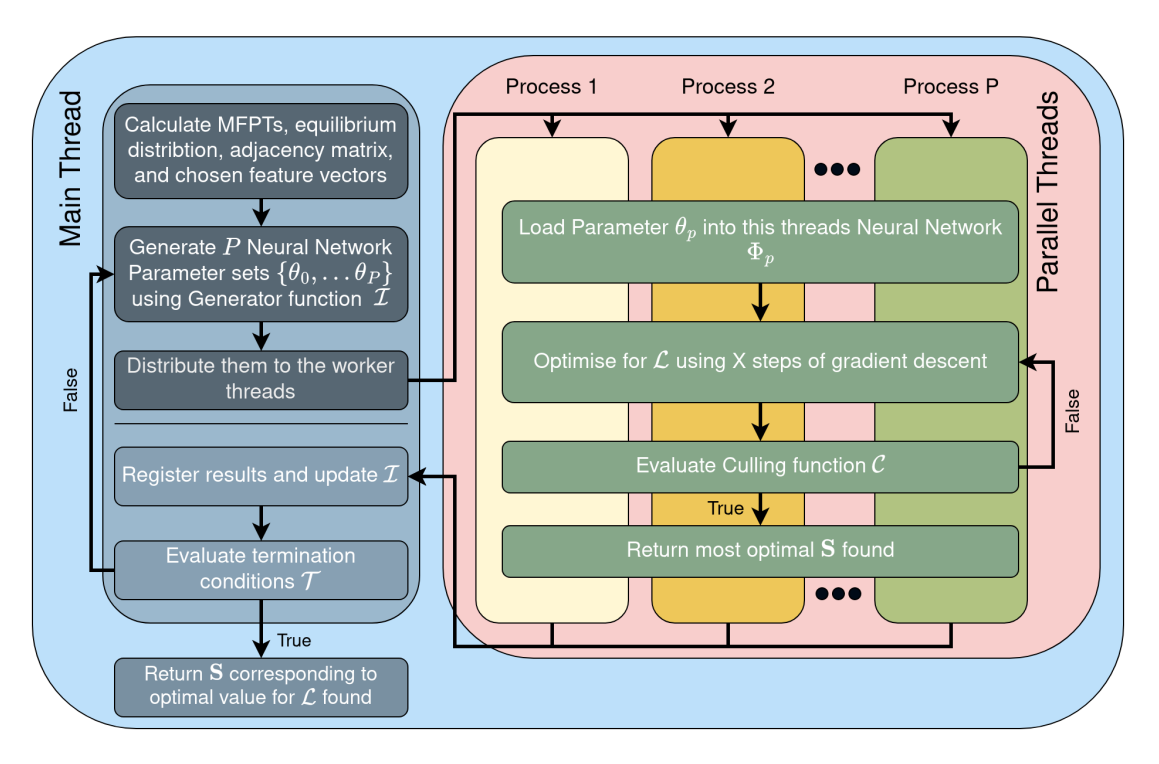


Figure 2. Schematic description of the algorithm used to train multiple networks in parallel, and the use of the general functions \mathcal{I} , \mathcal{C} , and \mathcal{T} .

To test the validity and effectiveness of using GNNs to cluster Markov chains, the method was first tested on synthetic kinetic graphs. Firstly, a simple stochastic block model (SBM) 54 was employed to generate random networks with 4 neighbourhoods. The initial set of networks used sampled inter-cluster connection probabilities from a Gaussian distribution scaled to be in the range [0, 0.25] and set intra-cluster probabilities to a constant 0.5. This led to networks with dense clusters, where the optimal partitioning always successfully separated them. We also designed SBM networks where the optimal clustering was less clear, sampling all connection probabilities from the same Gaussian as before. For both sets of examples, SBM networks with disconnected nodes were discarded, and the random-walk normalized Laplacian matrix, L, was used to generate rate matrices via:

$$\mathbf{L} = \mathbf{I} - \mathbf{A}\mathbf{D}^{-1} \tag{21}$$

Where I is the identity matrix, D is a matrix with the degrees of each node along the leading diagonal, and A is the adjacency matrix. Results on these synthetic graphs were compared to clusterings and respective ΔK values obtained from the PCCA+ method⁵⁵. Each SBM experiment trained 100 independently initialised models for 250 steps of gradient descent on 500 randomly generated graphs, ranging from N=150 to N=300 nodes in increments of 50.

To establish a baseline performance for all models on a single graph, the network was tested on a graph corresponding to a rate matrix derived from an analytical 1D potential simulation²⁹. The system consisted of 100 nodes distributed along the potential, which was comprised of 4 clear wells: 3 with 20 nodes and one with 40, with the optimal KC partitioning successfully separating all 4 into individual partitions. This example of a linear chain network architecture was chosen to test the network in situations where connectivity is limited. All 4 models were tested 1000 times on this example for 500 gradient descent steps each. A feature comparison was also performed on this system, where 1000 GraphSAGE + LD models were trained for 500 steps using each set of features described above.

Ultimately, the method was also tested on a network derived from MD data. We used the MSM benchmark system of PyEMMA⁵⁶ corresponding to 500 ns long implicit water MD simulations of a small

5-amino-acid system, which we refer to as the pentapeptide system. The simulation was first clustered into 250 states using K-means on tICA projected data, and then a Markov matrix was calculated 57,58 , which was used as the input to our method. Each experiment consisted of training 1000 models for 500 gradient descent steps to cluster the 250-state MSM into 5 states. As this example is the closest to examples derived from biomolecular simulations, we performed an additional hyper-parameter search for the optimal network architecture. For this, we again trained 1000 GraphSAGE + LD models for 500 steps while varying the number of layers in both the decoder and the encoder, along with d_{hidden} and d_{embed} . Additionally, we again performed a feature comparison in the same way as described earlier. We compared the results of this example to the PCCA+ and PVTC, our previous MCMC approach. 29

The neural networks and relevant code were implemented in Python 3.10.6 using PyTorch 2.0^{59} or Tensorflow. Network diagrams were made using the Netgraph library. To perform gradient descent steps the Adam optimizer was used with a learning rate of $1e^{-4}$. All networks used $d_{\rm embed}=32$ and $d_{\rm hidden}=64$, with 4 GNN layers in the encoder and 2 layers in the decoder, unless otherwise specified. Due to the numerical sensitivity and dependence of the MFPT calculation on accurate eigenvalues, 64-bit floats were used for all calculations and they were run on the CPU. Each experiment involved the simultaneous execution of 90 processes in parallel, with each process running on a single core.

4 RESULTS & DISCUSSION

Our GNN approach successfully found the optimal clustering for all SBM networks in the first set, where the clusters were well-defined, in 100 training runs or less. This matched the performance of the PCCA+ algorithm, confirming the viability of our method in trivial situations. Fig. 3 details the performance on the second set of SBM graphs featuring a more diverse range of networks. Our implementation identified partitionings which better optimised ΔK than the PCCA+. However, the improvement diminished as the number of nodes in the network increased, as often the clustering became clearer. We found that PCCA+ sometimes returned graphs without the specified number of clusters, and sometimes failed to find an effective partitioning when given unclear clusters. The stochastic nature of the GNN-based method however lends itself more to these systems where several viable partitionings have a low ΔK value. In these examples the optimal clustering is close to many other similar solutions, therefore it is helpful to evaluate many initialisations to evaluate most of the very low ΔK partitionings.

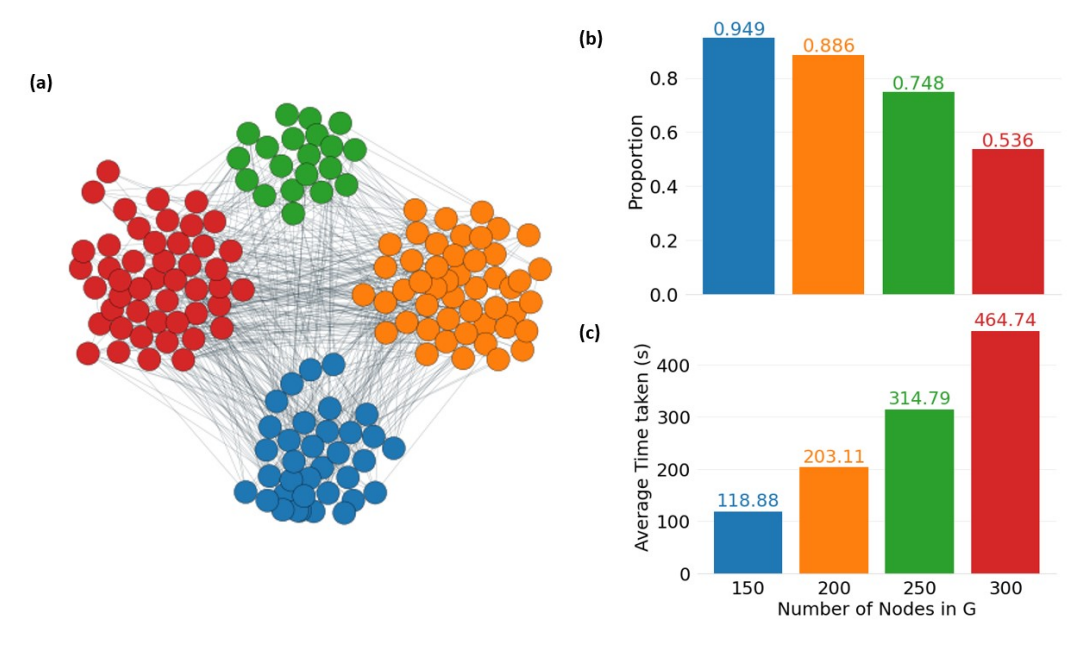


Figure 3. The performance of the SBM network clustering for randomly sampled cluster connection probabilities. (a) Example of a partitioning produced by the GNN optimisation. (b) and (c) Quantitative assessment of the method's performance over 100 runs for the 500 different networks. (b) The proportion of runs where the method yields a partitioning with a lower ΔK value than PCCA+. (c) The average time needed in seconds for one training run when limited to run on one 2.20GHz CPU core.

The 1D potential (Fig. 4a) was used to test our approach on sparse graphs where connectivity becomes limited, and the majority of effective ΔK partitionings lie in a small region of partitioning space. In this regime gradient descent steps can become less effective as the majority of initial partitions are far from the region of interest, and can be unable to escape their local minima. Fortunately, simply training more neural networks can alleviate the problem by providing a wider range of starting points for optimization. In future applications, an effective choice of the initialization function $\mathcal I$ could speed up convergence, whereby $\mathcal I$ can learn and then avoid initializing in uninteresting regions of parameter space. To further test whether different node features could improve the successful optimisation outcomes, we tested several additional node features, sampling the optimisation outcome 1000 times each. In total, we tested nine different node feature types: (i) adjacency matrix, (ii) the PCA vectors created from the adjacency matrix, (iii) rate matrix, (iv) the PCA vectors created from the rate matrix, (v) MFPTs (default in other examples), (vi) the PCA vectors created from the MFPT matrix, (vii) eigenvectors of the rate matrix, (viii) trainable embeddings, (ix) a neural network. The feature comparison results (Fig. 4b) show that it is possible to use improved node features, such as the adjacency matrix or a trainable embedding in this case, which achieve a much more successful optimisation for the 1D model potential-derived network.

Optimal partitionings are highly dependent on the connectivity of the graph. It becomes difficult to discriminate nodes at high energies (with low populations) based solely on the rate matrix, as these nodes have similar transitions. The adjacency matrix, however, provides more information on the node location in the global structure of the network, leading to a noticeable advantage. Our GNN implementation allows for simple changes to define the node features on a problem-specific basis, therefore giving the method additional viability across a wide range of MCs.

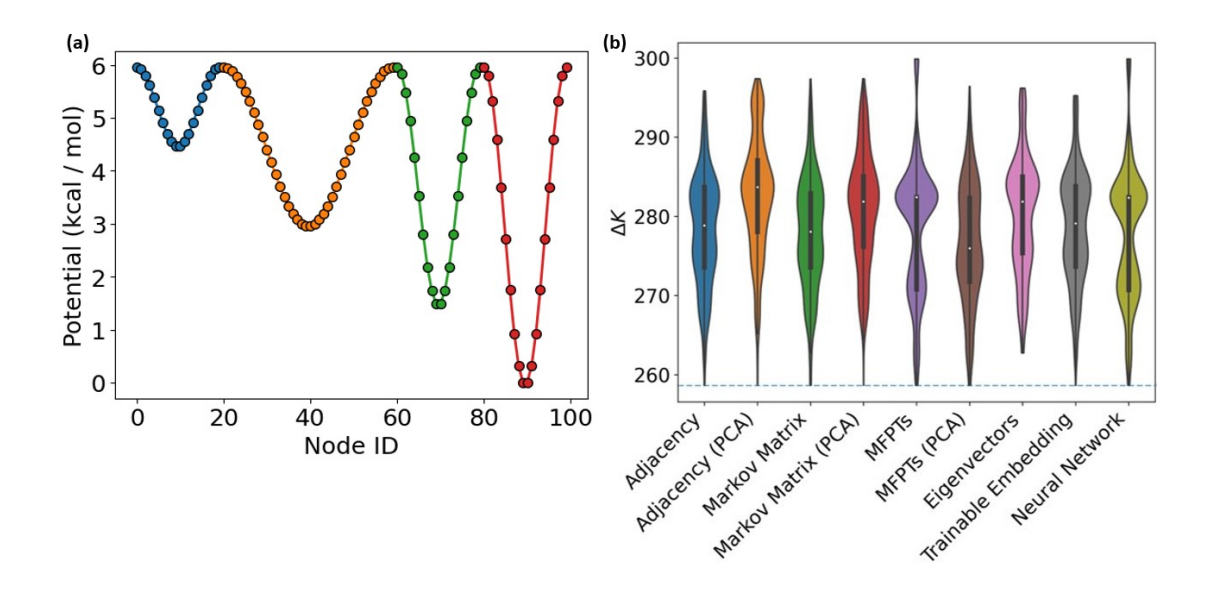


Figure 4. (a) 1D potential used for an example of a linear chain network. Nodes are coloured according to the most optimal 4-state clustering for the system. (b) Violin plots for feature comparisons on the 1D potential derived network. Each experiment was run 1000 times with each set of features. The corresponding distribution of final ΔK values is shown, along with a dotted blue line signifying the ΔK value of the optimal solution for each problem.

We also tested the four GNN architectures (Fig. 5) training 1000 models of each variety on the 1D potential, using the adjacency matrix as node features. We found that simpler models perform better at finding optimal partitionings over more complex models in this framework. Despite the better average performance larger models provided, none of them were able to find the optimal clustering over 1000 runs. The optimal clustering, however, is found consistently by both by the PVTC and the PCCA+ methods. The wide variance of the observed results showcases the poor ability of all models to optimize initial partitionings on this network when started from many regions of parameter space. The large magnitude of some solutions is indicative of a partitioning problem where there is only a small region of interest in partitioning space and larger models like the GATv2 and TD models struggle to find this parameter space, possibly due to the more complex and unclear gradients calculated when the node embeddings are more co-dependent and additional resources and required to train the extra parameters.

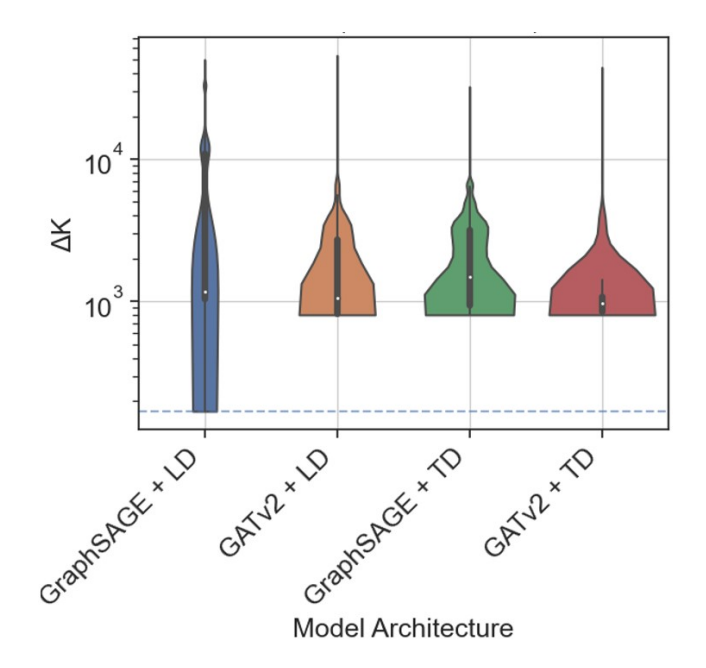


Figure 5. The distribution of ΔK values from training 1000 copies of each neural network architecture on the 1D potential derived network. A logarithmic scale is used to highlight the large differences between the different models. The blue dashed line indicates the value associated with the optimal clustering for this system.

Table 1. Network architecture comparison for the 1D potential derived network. The four network architectures are compared in terms of the mean (standard deviation) and minimum for 1000 experiments, along with the percentage of times the optimal solution was found.

Model Name	Mean	Minimum	Global Minimum Accuracy
GraphSAGE + LD	$5884.74 (\pm 8372.62)$	169.69	5.6%
GATv2 + LD	1988.50 (\pm 2696.11)	806.48	0.0%
GraphSAGE + TD	$2201.59 (\pm 1796.45)$	806.48	0.0%
GATv2 + TD	$1508.19 (\pm 2728.35)$	806.48	0.0%

However, examples derived from numerical simulations of bio-molecular systems often result in noisy derived MCs with dense connections, such as in the pentapeptide case. Here, as shown in Fig. 7 and Table 2, the simplest GraphSAGE and linear decoder method outperforms all other methods similarly to the 1D example above. The PVTC method and PCCA+ also cannot correctly identify the optimal clustering. In this example our method finds the optimal clustering less frequently than in the synthetic examples of SBM networks. This could be due to the increased number of low ΔK partitionings available, which provide many local minima, which are more difficult to escape. MCMC methods struggle with this same issue, having difficulty finding the relevant areas of partitioning space. The dense nature of the clusters means, it is difficult for PCCA+-based methods to identify the most optimal clustering do not differ much in terms of meta-stability. Nevertheless, the optimal PCCA+ clustering is remarkably close to the optimal Kemeny constant-based clustering. The larger models suffer from a vanishing gradient due to the heavily conditional nature of optimizing all node partition probabilities at the same time, resulting in an inability to find the optimal clustering even once while nevertheless providing a better result on average than the GraphSAGE and LD model. Still, they are outclassed by the PCCA+, and all but the GraphSAGE with transformer decoder model provide worse performance than PVTC, highlighting the efficiency of simpler networks for this kind of task. While further analysis of learning rate adjustments could provide an effective solution to train larger and more complex models on this problem, it is clear that training simple networks is both quicker and more reliable to find the optimal clustering. Feature comparisons on the GraphSAGE + LD example show the success of the method in finding the optimal partitioning over 1000 individual runs with all features tested except for using the eigenvectors (Fig. 4b). MFPTs show the best performance here, finding the optimal solution the greatest number of times. Most likely due to the computational simplicity in finding effective mappings from the MFPTs to optimized partitionings, as the value of Eq. (20) directly depends upon them. The poor performance of the eigenvectors is most likely down to numerical stability, as some of them are very small 64-bit floats.

One advantage MCMC methods such as the PVTC have over our method is the ability to be initialised from any arbitrary partitioning. The results shown are for the PVTC when given no initial clustering information, however, when the method is initialised from the PCCA+ solution it consistently finds the optimal solution in all occasions. To try to replicate this behaviour, we changed our initialisation function $\mathcal I$ to pretrain the models to replicate the PCCA+ solution using mean-squared error loss that is minimal for the optimal PCCA+ solution. Once the GNN is trained to this specific loss function and identifies the PCCA+ clustering, it is then further trained to the Kemeny loss of Eq. (20). This pretraining, however, did not improve performance of the GNN optimisation (data not shown).

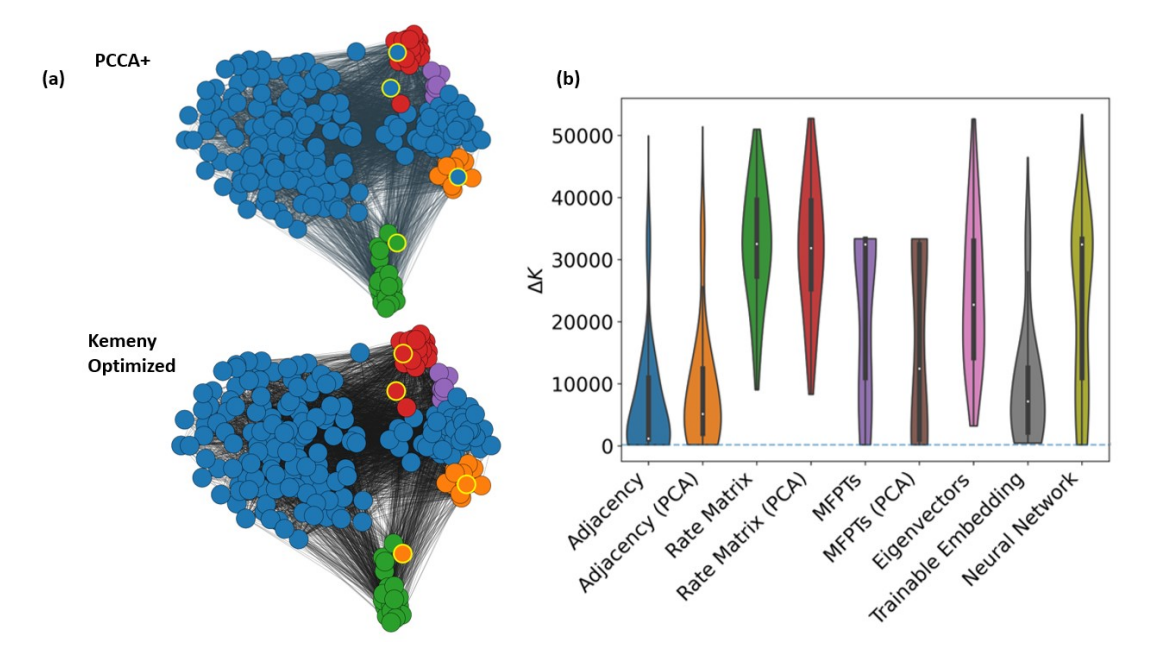


Figure 6. (a) Comparison of the PCCA+ solution with the optimal ΔK clustering for the pentapeptide system. Networks are displayed using a force-directed layout weighted with the MFPTs. Nodes which differ between the two clusters are highlighted with a yellow border. (b) Violin plot distributions for 1000 experiments with each set of nine features. The corresponding distribution of final ΔK values is shown as a violin plot, along with a blue dashed line for the optimal ΔK value.

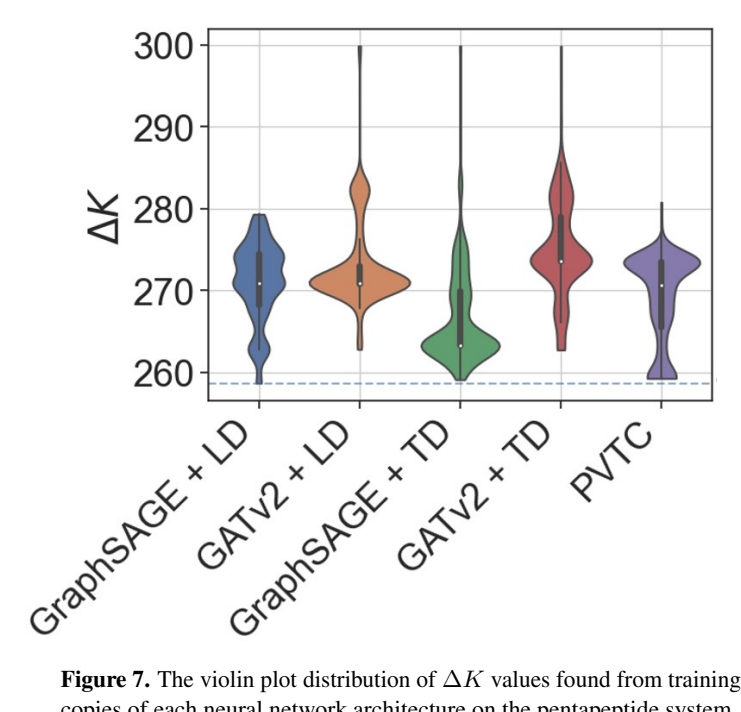


Figure 7. The violin plot distribution of ΔK values found from training 1000 copies of each neural network architecture on the pentapeptide system. The blue dashed line indicates the value associated with the optimal clustering.

Table 2. Network architecture comparison for the pentapeptide system. The four network architectures are compared in terms of the mean (standard deviation) and minimum for 1000 experiments, along with the percentage of times the optimal solution was found.

Model Name	Mean	Minimum	Global Minimum Accuracy
GraphSAGE + LD	$271.03 (\pm 4.80)$	258.67	2.8%
GATv2 + LD	$273.28 (\pm 5.71)$	262.81	0.0%
GraphSAGE + TD	266.66 (\pm 5.94)	259.098	0.0%
GATv2 + TD	$274.92 (\pm 5.81)$	262.74	0.0%

We also performed a hyperparameter search on our GNN network to identify the optimal depth and network sizes for the training. The parameter search was performed on the pentapeptide example. It highlights the problem that the network's effectiveness is highly dependent upon the chosen hyperparameters of the neural network and the size of the network. The best parameter space for a given problem must be sufficiently large to be able to express the wide multitude of possible S matrices, while also being small enough to allow for effective optimisation in a feasible time. This is highlighted by the poorer performance of most networks featuring four linear layers in the decoder, where most of the time the method either fails to find the optimal solution or does so rarely it is classified as an outlier. Future work can further verify whether a varying or learnable adjustment to the learning rate could provide a reasonable improvement, as this would allow networks to more efficiently probe the relevant regions of parameter space. Alternatively, further work could evaluate if it is possible to quantify the relationship between the size of the graph being clustered and the most optimal network size.

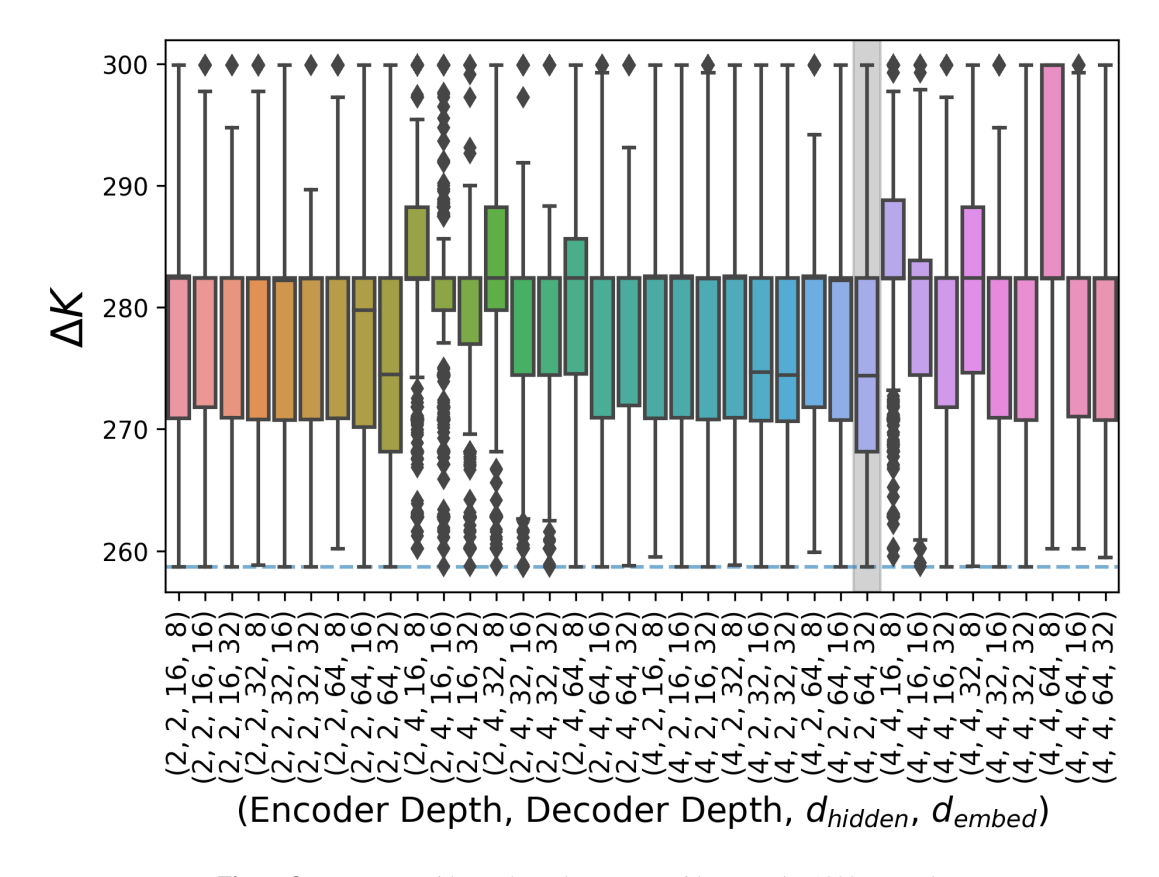


Figure 8. Parameter grid search on the pentapeptide example. 1000 networks were initialised for each set of parameters, and the resulting ΔK distribution is shown. The grey background indicates the parameters identified as optimal.

5 CONCLUSION

We describe a GNN-based network clustering optimisation method, which uses the computing infrastructure and tooling that has risen around GNNs to provide a working basis for difficult optimization problems on graphs. The benefits are numerous, as GNNs provide an ample Ansatz for beginning optimization for partitioning phenomena in situations where otherwise finding an efficient representation for the task proves difficult.

We provide a novel implementation of a GP approach to cluster graphs based on kinetic optimization criteria. Here we use the Kemeny constant to obtain metastable kinetically optimal clusters. We outline a general methodology for training GNNs to optimize graph partitionings and compare the performance of four different architectures across three different kinetic network types, using several different node features. Our results show that smaller and simpler networks often show superior performance in our test cases, as larger networks become more difficult to optimize, and often cannot find the optimal solutions. Testing the method on SBM graphs with clear clusters, we can attain similar results to existing methods, such as PCCA+. Frequently GNN optimizations even outperform the PCCA+ solution in terms of ΔK on SBM graphs with ill-defined clusters. However, SBM networks are generally easier to cluster compared to networks defined from kinetic processes. A linear chain corresponding to an analytic 1D free energy profile also poses a difficult task for GNNs due to the low connectivity, while PCCA+ in this case can produce the optimal solution. We show how we can adapt the node features the GNN uses and the number of runs to alleviate this problem, and improve the performance. However, the optimal clustering is only found in about 5% of the attempts in only one GNN architecture, and therefore improving the reliability of the method still requires future work. The outline of our general methodology, introducing the strategy defining generator \mathcal{I} , culling \mathcal{C} , and termination \mathcal{T} functions, provides an ample framework for future work in this direction. Our MD-simulation derived MSM for a pentapeptide has an optimal ΔK clustering

that seems to better capture metastable states than the PCCA+-derived clusters. Only one of the four architectures can find this optimal solution in less than 3% of the time, highlighting the problem of GNNs, which further work on $\mathcal I$ function can hopefully provide a solution for. Additionally, GNNs do not provide a straightforward way to initialize the search from a close-to-optimal solution, which makes the PVTC algorithm much more efficient.

In summary, we have shown the validity of using GNNs to effectively cluster MCs and described a general framework which is straightforward to generalize to both different cluster optimization criteria and graph-like structures. We have proposed a GNN-based methodology for GP that can be further generalized and explored in future work. It remains to be seen how to implement more complex parameter space sampling strategies to aid the identification of more optimal solutions, taking inspiration from similar techniques used for enhanced sampling in MD.

6 ACKNOWLEDGMENTS

We thank Dr. Alessia Annibale for helpful suggestions, Madhav Sharma for his feedback on the manuscript, and Bin Liang for his initial contributions to pretraining. The authors acknowledge funding from ERC Starting Grant (Project 757850 BioNet) and EPSRC (grant no. EP/R013012/1). This project made use of time on ARCHER granted via the UK High-End Computing Consortium for Biomolecular Simulation, HECBioSim (http://hecbiosim.ac.uk). The authors acknowledge the use of the UCL Myriad High Performance Computing Facility (Myriad@UCL), and associated support services, in the completion of this work.

REFERENCES

- [1] Hiroshi Okamoto and Xule Qiu. "Detecting hierarchical organization of pervasive communities by modular decomposition of Markov chain". In: *Scientific Reports* 12.1 (2022), p. 20211.
- [2] Philipp Von Hilgers and Amy N Langville. "The five greatest applications of Markov chains". In: *Proceedings of the Markov Anniversary meeting*. Boston Press Boston, MA. 2006, pp. 155–158.
- [3] Conrad Sanderson and Simon Guenter. "Short text authorship attribution via sequence kernels, Markov chains and author unmasking: An investigation". In: *Proceedings of the 2006 Conference on Empirical Methods in Natural Language Processing*. 2006, pp. 482–491.
- [4] Sophie Schbath. "An overview on the distribution of word counts in Markov chains". In: *Journal of Computational Biology* 7.1-2 (2000), pp. 193–201.
- [5] Lawrence Page et al. *The pagerank citation ranking: Bring order to the web*. Tech. rep. Technical report, stanford University, 1998.
- [6] Henri Berthiaux and Vadim Mizonov. "Applications of Markov chains in particulate process engineering: a review". In: *The Canadian journal of chemical engineering* 82.6 (2004), pp. 1143–1168.
- [7] Diwakar Shukla et al. "Markov State Models Provide Insights into Dynamic Modulation of Protein Function". In: *Accounts of Chemical Research* 48.2 (2015). PMID: 25625937, pp. 414–422. DOI: 10.1021/ar5002999. eprint: https://doi.org/10.1021/ar5002999. URL: https://doi.org/10.1021/ar5002999.
- [8] William C. Swope, Jed W. Pitera, and Frank Suits. "Describing Protein Folding Kinetics by Molecular Dynamics Simulations. 1. Theory". In: *The Journal of Physical Chemistry B* 108.21 (2004), pp. 6571–6581. DOI: 10.1021/jp037421y. eprint: https://doi.org/10.1021/jp037421y. URL: https://doi.org/10.1021/jp037421y.
- [9] Nina Singhal, Christopher D. Snow, and Vijay S. Pande. "Using path sampling to build better Markovian state models: Predicting the folding rate and mechanism of a tryptophan zipper beta hairpin". In: *The Journal of Chemical Physics* 121.1 (June 2004), pp. 415–425. ISSN: 0021-9606. DOI: 10.1063/1.1738647. eprint: https://pubs.aip.org/aip/jcp/article-pdf/121/1/415/10858528/415_1_online.pdf. URL: https://doi.org/10.1063/1.1738647.
- [10] Albert C Pan and Benoit Roux. "Building Markov state models along pathways to determine free energies and rates of transitions". In: *The Journal of chemical physics* 129.6 (2008).

- [11] Linda Martini et al. "Variational Identification of Markovian Transition States". In: *Phys. Rev. X* 7 (3 Sept. 2017), p. 031060. DOI: 10.1103/PhysRevX.7.031060. URL: https://link.aps.org/doi/10.1103/PhysRevX.7.031060.
- [12] Thomas J Lane et al. "Markov state model reveals folding and functional dynamics in ultra-long MD trajectories". In: *Journal of the American Chemical Society* 133.45 (2011), pp. 18413–18419.
- [13] Gregory R Bowman et al. "Discovery of multiple hidden allosteric sites by combining Markov state models and experiments". In: *Proceedings of the National Academy of Sciences* 112.9 (2015), pp. 2734–2739.
- [14] Andreas Mardt et al. "VAMPnets for deep learning of molecular kinetics". In: *Nature communications* 9.1 (2018), p. 5.
- [15] Sunhwan Jo et al. "Leveraging the information from Markov state models to improve the convergence of umbrella sampling simulations". In: *The journal of physical chemistry B* 120.33 (2016), pp. 8733–8742.
- [16] Brooke E. Husic and Vijay S. Pande. "Markov State Models: From an Art to a Science". In: *Journal of the American Chemical Society* 140.7 (2018). PMID: 29323881, pp. 2386–2396. DOI: 10.1021/jacs.7b12191. eprint: https://doi.org/10.1021/jacs.7b12191. URL: https://doi.org/10.1021/jacs.7b12191.
- [17] Peter Deuflhard and Marcus Weber. "Robust Perron cluster analysis in conformation dynamics". In: *Linear algebra and its applications* 398 (2005), pp. 161–184.
- [18] Gerhard Hummer and Attila Szabo. "Optimal dimensionality reduction of multistate kinetic and Markov-state models". In: *The Journal of Physical Chemistry B* 119.29 (2015), pp. 9029–9037.
- [19] Nicolae-Viorel Buchete and Gerhard Hummer. "Coarse master equations for peptide folding dynamics". In: *The Journal of Physical Chemistry B* 112.19 (2008), pp. 6057–6069.
- [20] Bernhard Reuter, Konstantin Fackeldey, and Marcus Weber. "Generalized Markov modeling of nonreversible molecular kinetics". In: *The Journal of Chemical Physics* 150.17 (2019), p. 174103. DOI: 10.1063/1.5064530.
- [21] Yuxing Peng et al. "OpenMSCG: A Software Tool for Bottom-Up Coarse-Graining". In: *The Journal of Physical Chemistry B* 127.40 (2023), pp. 8537–8550.
- [22] Jiang Wang et al. "Machine learning of coarse-grained molecular dynamics force fields". In: ACS central science 5.5 (2019), pp. 755–767.
- [23] Yan Li and Zigang Dong. "Effect of clustering algorithm on establishing Markov state model for molecular dynamics simulations". In: *Journal of chemical information and modeling* 56.6 (2016), pp. 1205–1215.
- [24] Daniel Nagel, Sofia Sartore, and Gerhard Stock. "Toward a Benchmark for Markov State Models: The Folding of HP35". In: *The Journal of Physical Chemistry Letters* 14.31 (2023), pp. 6956–6967.
- [25] Susanna Röblitz and Marcus Weber. "Fuzzy spectral clustering by PCCA+: application to Markov state models and data classification". In: *Advances in Data Analysis and Classification* 7 (2013), pp. 147–179.
- [26] Barbu and Zhu. "Graph partition by Swendsen-Wang cuts". In: *Proceedings Ninth IEEE International Conference on Computer Vision*. IEEE. 2003, pp. 320–327.
- [27] David F Anderson and Desmond J Higham. "Multilevel Monte Carlo for continuous time Markov chains, with applications in biochemical kinetics". In: *Multiscale Modeling & Simulation* 10.1 (2012), pp. 146–179.
- [28] Zhao Tang Luo, Huiyan Sang, and Bani Mallick. "A Bayesian contiguous partitioning method for learning clustered latent variables". In: *The Journal of Machine Learning Research* 22.1 (2021), pp. 1748–1799.
- [29] Vladimir Koskin et al. "Variational kinetic clustering of complex networks". In: *The Journal of Chemical Physics* 158.10 (Mar. 2023), p. 104112. ISSN: 0021-9606. DOI: 10.1063/5.0105099. eprint: https://pubs.aip.org/aip/jcp/article-pdf/doi/10.1063/5.0105099/16791340/104112_1_online.pdf. URL: https://doi.org/10.1063/5.0105099.

- [30] Uri Shaham et al. "Spectralnet: Spectral clustering using deep neural networks". In: *arXiv preprint arXiv:1801.01587* (2018).
- [31] Tatsuro Kawamoto, Masashi Tsubaki, and Tomoyuki Obuchi. "Mean-field theory of graph neural networks in graph partitioning". In: *Advances in Neural Information Processing Systems* 31 (2018).
- [32] Renjie Liao et al. "Graph partition neural networks for semi-supervised classification". In: *arXiv* preprint arXiv:1803.06272 (2018).
- [33] Azade Nazi et al. "GAP: Generalizable Approximate Graph Partitioning Framework". In: *CoRR* abs/1903.00614 (2019). arXiv: 1903.00614. URL: http://arxiv.org/abs/1903.00614.
- [34] Anton Tsitsulin et al. "Graph Clustering with Graph Neural Networks". In: *CoRR* abs/2006.16904 (2020). arXiv: 2006.16904. URL: https://arxiv.org/abs/2006.16904.
- [35] Nina Singhal and Vijay S. Pande. "Error analysis and efficient sampling in Markovian state models for molecular dynamics". In: *The Journal of Chemical Physics* 123.20 (2005), p. 204909. DOI: 10.1063/1.2116947. eprint: https://doi.org/10.1063/1.2116947. URL: https://doi.org/10.1063/1.2116947.
- [36] Mark EJ Newman. "Modularity and community structure in networks". In: *Proceedings of the national academy of sciences* 103.23 (2006), pp. 8577–8582.
- [37] Roger Guimera, Marta Sales-Pardo, and Luis A Nunes Amaral. "Modularity from fluctuations in random graphs and complex networks". In: *Physical Review E* 70.2 (2004), p. 025101.
- [38] Benjamin H Good, Yves-Alexandre De Montjoye, and Aaron Clauset. "Performance of modularity maximization in practical contexts". In: *Physical review E* 81.4 (2010), p. 046106.
- [39] Gaurav Agarwal and David Kempe. "Modularity-maximizing graph communities via mathematical programming". In: *The European Physical Journal B* 66 (2008), pp. 409–418.
- [40] Tom Leighton and Satish Rao. "Multicommodity max-flow min-cut theorems and their use in designing approximation algorithms". In: *Journal of the ACM (JACM)* 46.6 (1999), pp. 787–832.
- [41] Chris HQ Ding et al. "A min-max cut algorithm for graph partitioning and data clustering". In: *Proceedings 2001 IEEE international conference on data mining*. IEEE. 2001, pp. 107–114.
- [42] Lars Hagen and Andrew Kahng. "Fast spectral methods for ratio cut partitioning and clustering". In: 1991 IEEE international conference on computer-aided design digest of technical papers. IEEE Computer Society. 1991, pp. 10–11.
- [43] Guy Even et al. "Fast approximate graph partitioning algorithms". In: *SIAM Journal on Computing* 28.6 (1999), pp. 2187–2214.
- [44] Konstantin Andreev and Harald Räcke. "Balanced graph partitioning". In: *Proceedings of the sixteenth annual ACM symposium on Parallelism in algorithms and architectures*. 2004, pp. 120–124.
- [45] Robert Krauthgamer, Joseph Naor, and Roy Schwartz. "Partitioning graphs into balanced components". In: *Proceedings of the twentieth annual ACM-SIAM symposium on Discrete algorithms*. SIAM. 2009, pp. 942–949.
- [46] Adam Kells et al. "Correlation functions, mean first passage times, and the Kemeny constant". In: *The Journal of Chemical Physics* 152.10 (Mar. 2020), p. 104108. DOI: 10.1063/1.5143504. URL: https://doi.org/10.1063%5C%2F1.5143504.
- [47] Justin Gilmer et al. "Neural Message Passing for Quantum Chemistry". In: *CoRR* abs/1704.01212 (2017). arXiv: 1704.01212. URL: http://arxiv.org/abs/1704.01212.
- [48] William L. Hamilton, Rex Ying, and Jure Leskovec. "Inductive Representation Learning on Large Graphs". In: *CoRR* abs/1706.02216 (2017). arXiv: 1706.02216. URL: http://arxiv.org/abs/1706.02216.
- [49] Shaked Brody, Uri Alon, and Eran Yahav. "How Attentive are Graph Attention Networks?" In: CoRR abs/2105.14491 (2021). arXiv: 2105.14491. URL: https://arxiv.org/abs/2105.14491.

- [50] Tomas Mikolov et al. "Distributed representations of words and phrases and their compositionality". In: *Advances in neural information processing systems* 26 (2013).
- [51] Günter Klambauer et al. "Self-Normalizing Neural Networks". In: *CoRR* abs/1706.02515 (2017). arXiv: 1706.02515. URL: http://arxiv.org/abs/1706.02515.
- [52] Kaiming He et al. "Delving deep into rectifiers: Surpassing human-level performance on imagenet classification". In: *Proceedings of the IEEE international conference on computer vision*. 2015, pp. 1026–1034.
- [53] Xavier Glorot and Yoshua Bengio. "Understanding the difficulty of training deep feedforward neural networks". In: *Proceedings of the thirteenth international conference on artificial intelligence and statistics*. JMLR Workshop and Conference Proceedings. 2010, pp. 249–256.
- [54] Emmanuel Abbe. "Community detection and stochastic block models: recent developments". In: *Journal of Machine Learning Research* 18.177 (2018), pp. 1–86.
- [55] Susanna Kube and Marcus Weber. "A coarse graining method for the identification of transition rates between molecular conformations". In: *The Journal of chemical physics* 126.2 (2007).
- [56] Martin K Scherer et al. "PyEMMA 2: A software package for estimation, validation, and analysis of Markov models". In: *Journal of chemical theory and computation* 11.11 (2015), pp. 5525–5542.
- [57] Christian R Schwantes and Vijay S Pande. "Improvements in Markov state model construction reveal many non-native interactions in the folding of NTL9". In: *Journal of chemical theory and computation* 9.4 (2013), pp. 2000–2009.
- [58] Guillermo Pérez-Hernández et al. "Identification of slow molecular order parameters for Markov model construction". In: *The Journal of chemical physics* 139.1 (2013).
- [59] Adam Paszke et al. "Pytorch: An imperative style, high-performance deep learning library". In: *Advances in neural information processing systems* 32 (2019).
- [60] Martín Abadi et al. *TensorFlow: Large-Scale Machine Learning on Heterogeneous Systems*. Software available from tensorflow.org. 2015. URL: https://www.tensorflow.org/.
- [61] Paul J. N. Brodersen. "Netgraph: Publication-quality Network Visualisations in Python". In: *Journal of Open Source Software* 8.87 (2023), p. 5372. DOI: 10.21105/joss.05372. URL: https://doi.org/10.21105/joss.05372.
- [62] Diederik P Kingma and Jimmy Ba. "Adam: A method for stochastic optimization". In: *arXiv* preprint arXiv:1412.6980 (2014).